Atomic and electronic structure of silicon nanocrystals embedded in a silica matrix

2008 J. Phys.: Condens. Matter 20 455209

(http://iopscience.iop.org/0953-8984/20/45/455209)

J. Phys.: Condens. Matter **20** (2008) 455209 (8pp) doi:10.1088/0953-8984/20/45/455209

Atomic and electronic structure of silicon nanocrystals embedded in a silica matrix

Ngoc Bich Nguyen[1], Christian Dufour[1] and Sebastien Petit[2]

[1] Centre de Recherche sur les Ions, les Matériaux et la Photonique, 6 boulevard Marechal Juin, 14050 Caen Cedex, France
[2] Laboratoire de Cristallographie et Sciences des Matériaux, 6 boulevard Marechal Juin, 14050 Caen Cedex, France

Received 16 June 2008, in final form 5 September 2008
Published 13 October 2008
Online at stacks.iop.org/JPhysCM/20/455209

Abstract

The atomic structures and the optical and electronic properties of silicon nanocrystals (nc-Si) in a β cristobalite matrix are studied using DFT calculations provided by the AIMPRO code. Five atomic models are considered (two nanocrystal diameters of 5.6 and 11 Å with and without interface defects). After total relaxation, the mean Si–Si distances in nc-Si are found to be 6% higher than those in perfect bulk silicon. The optical and electronic properties are influenced by many parameters, among which are the nanograin density and size. The quantum confinement effect is demonstrated by the increase of energy gap when decreasing nanograin size. The energy gap of nc-Si is adjusted by using B3LYP functional calculations; the energy gap of 5.6 Å nc-Si is found to be equal to 3.4 eV while that of 11 Å nc-Si is equal to 3.1 eV. In the band structure, the levels due to nc-Si appear in the forbidden band of SiO_2. The electronic density of these levels is presented in 3D. A redshift is observed in the optical absorption spectrum as the nc-Si size increases, and the absorbance of nc-Si/SiO_2 is proportional to the nanograin density. The system is more stable as the distance between nanograins increases. We have also studied two kinds of nc-Si/SiO_2 interface defects (Si–O–Si and Si=O bonds). It is found that the Si–O–Si bridge bond leads to the most stable configuration. The presence of Si=O double bonds reduces the nc-Si energy gap and leads to a redshift in the absorption spectrum. The Si–O–Si bonds produce the inverse effect, i.e. an energy gap increase associated with a blueshift in the absorption spectrum.

(Some figures in this article are in colour only in the electronic version)

1. Introduction

The use of silicon in optical applications was long limited by the small and indirect band gap until visible photoluminescence (PL) was discovered in porous Si two decades ago [1]. Since then, materials composed of silicon nanocrystals (nc-Si) embedded in a silica matrix (SiO_2) have been produced by numerous techniques such as plasma enhanced chemical vapor deposition [2], reactive magnetron sputtering [3], ion implantation [4, 5], molecular beam epitaxy [6] and inverse micelle based chemical reactions [7]. All the cited materials exhibit intense visible PL with respect to porous silicon [8]. It is now commonly admitted that the peculiar photoluminescence properties of nc-Si are due to the quantum confinement of the generated photocarriers within the nc-Si as well as to specific electronic states localized at the nc-Si/SiO_2 interface [9–11].

The modeling of an nc-Si embedded in the SiO_2 matrix requires us to deal with hundreds of atoms since the experimental nc-Si diameter is in the 5–30 Å range. The huge number of atoms is the main reason why the theoretical works on nanograins are principally based on tight binding calculations [12], potential approaches [13, 14] and calculations using the density functional theory (DFT) on hydrogen passivated Si nanocrystals [15–18]. Thus, there are still only a few DFT calculations [2, 19] on embedded and realistic nanograins. The first theoretical works on such a system were performed by Delerue *et al* [20]. Within the framework of tight binding calculations combined more recently with the GW + Bethe–Salpeter equation, values of optical gap of silicon nanocrystals were proposed. Besides, they showed that one particle theory (like the local density approximation (LDA) and generalized gradient approximation

(GGA)) seems quite accurate to evaluate the excitonic gap for nanocrystals larger than 6 Å [21]. Structural properties of large nanograins (around 30 Å) were investigated with Monte Carlo simulation using the force field model [13]. In such an approach, no Si=O bond can be formed at the grain surface and the authors concluded that the low energy geometries of the nc-Si/SiO_2 interface contain Si–O–Si bridge bonds. Moreover, the fraction of bridge bonds sharply decreases from 62% to 33% when the nc-Si size decreases from 35 to 10 Å. Recently, the use of the molecular dynamic approach allows Djurabekova *et al* [14] to observe Si=O and dangling bonds on large nanograins embedded in amorphous silica. Most of the DFT calculations were only performed on hydrogen passivated Si nanocrystals with or without interface defects. It is worth noticing that the relaxed atomic positions do not take into account the SiO_2 matrix. The main result is that the Si–O–Si bridge and not the Si=O bond leads to the lowest energy structure. On the basis of these geometries, accurate calculations of optical properties have been performed using the GW + Bethe–Salpeter equation [18] and TDDFT [17]. Daldosso *et al* [2] were the first to propose a DFT geometry of a small nanograin of 10 Si atoms embedded in silica. However, the study of defects on the surface was not proposed.

In the present paper, we realize the theoretical simulations of nc-Si embedded in a crystalline silica matrix and propose to study the influence of the nc-Si size, the nc-Si density and the presence of surface defects on the electronic properties. Section 2 deals with the computational method. In section 3, we present five models of nc-Si embedded in β cristobalite with different nanograin densities and sizes as well as various interface defects in order to describe the influence of these parameters on the electronic and optical properties. This crystalline form has been chosen since it is the one closer to the crystalline silicon structure and this ensures one of the simplest Si/SiO_2 interfaces. The results for atomic, electronic and optical properties of nc-Si/SiO_2 will be presented in sections 4 and 5.

2. Computational method

We use density functional theory under the local density approximation as implemented in the AIMPRO package [22, 23] for all the supercell calculations and several specific molecular calculations. In this approach, we use Gaussian basis sets and pseudopotentials developed by Hartwigsen *et al* [24]. Each of the 2s and the three 2p valence orbitals of Si and O atoms is described by two contractions of four Gaussians. Besides, a d-Gaussian type polarization function is added for each atom. The exponents and coefficients of this basis set have been optimized in α quartz SiO_2. Using this basis, β cristobalite lattice parameter is correctly evaluated as 7.35 Å which is 2.6% larger than the experimental value (7.16 Å [25]). Moreover, we have correctly calculated the heat of formation H_f which is the difference between the energies of one Si and two O atoms in their standard states and the energy of a SiO_2 group in β cristobalite. We found $H_f = 9.26$ eV, which is close to the experimental value (9.16 eV) [26]. Brillouin zone sampling is integrated using the MP scheme proposed by Monkhorst and Pack [27]. We check the energy convergence as a function of the number of k points in order to choose an optimal k point grid for each system. We realize the total relaxation using a two-step procedure: (i) the atomic positions are relaxed keeping fixed the cell dimensions and the cell angles and (ii) we optimize the lattice parameters keeping atom positions fixed at the values found at the end of step (i). This procedure is repeated until convergence of the geometry. Once we have obtained the totally relaxed structure, we determine the band structure along the usual XMRΓMk point path for cubic structures: X(0.5, 0, 0), M(0.5, 0.5, 0), R(0.5, 0.5, 0.5), Γ(0, 0, 0).

The electronic energy loss spectroscopy (EELS) is simulated by calculating $-\mathrm{Im}(\epsilon(E)^{-1})$ where ϵ is the dielectric function and E is the energy loss [28]. The imaginary part of the dielectric function is calculated in the long-wavelength dipole approximation. The real part of the dielectric function is obtained through a Kramers–Kronig transformation. The EELS spectra are broadened using a Lorentzian function.

The formation energy of an nc-Si in SiO_2 informs us on the stability of each modelized structure. Since these structures contain only neutral defects, the formation energy can be evaluated as described by Eberlein *et al* [29]: $E_f = E_{tot} - n_{Si}\mu_{Si} - n_O\mu_O$, where E_{tot} is the total energy of the supercell containing n_{Si} silicon atoms and n_O oxygen atoms. μ_{Si} and μ_O are the chemical potentials of Si and O. The chemical potentials satisfy the condition that $\mu_{Si} + 2\mu_O$ is equal to the energy of a SiO_2 group in β cristobalite. Silicon nanograins are produced from substoichiometric SiO_x films containing excess silicon atoms [2], so that nc-Si/SiO_2 can be considered as a Si-rich system. The chemical potentials are then $\mu_{Si} = \mu_{Si}^{bulk}$ and $2\mu_O = \mu_{O_2} - H_f$, where μ_{Si}^{bulk} is the energy of a Si atom in bulk silicon and μ_{O_2} is the oxygen molecule energy in the triplet state. $\mu_{Si} = -3.952\,67$ (au), $\mu_O = -16.106\,29$ (au) and the evaluated heat of formation is H_f. These values are used to calculate the formation energy of nc-Si in $SiO_2\beta$ cristobalite.

On the clusters built from the Si nanograins embedded in SiO_2 (found by LDA calculations in this paper), we performed molecular calculations with the CRYSTAL06 package [30] within the B3LYP approximation. The HOMO/LUMO (highest occupied Kohn–Sham orbital/lowest unoccupied Kohn–Sham orbital) energy differences were evaluated using the basis sets denoted 66-21G* for the silicon atoms [31], 6-31G* for the oxygen atoms [32] and 31G* for the hydrogen atoms [32].

3. Si nanocrystal structures

We study five models of nc-Si embedded in SiO_2 β cristobalite. A single β-SiO_2 cubic cell contains eight SiO_2 units. β cristobalite has a diamond-like symmetry ($Fd3m$). An oxygen atom is located at the center of two silicon atoms so that the Si–O–Si bond angle is equal to 180°. The experimental lattice constant is 7.16 Å [25].

3.1. $Si_{10}(2 \times 2 \times 2)$

To model a silicon nanograin embedded in the SiO_2 matrix, we design a cubic 2 × 2 × 2 supercell whose cell side is equal

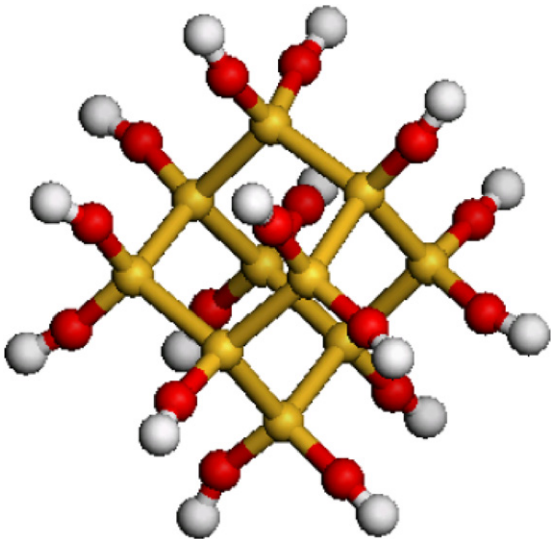

Figure 1. Structure of cluster $Si_{10}(OH)_{16}$.

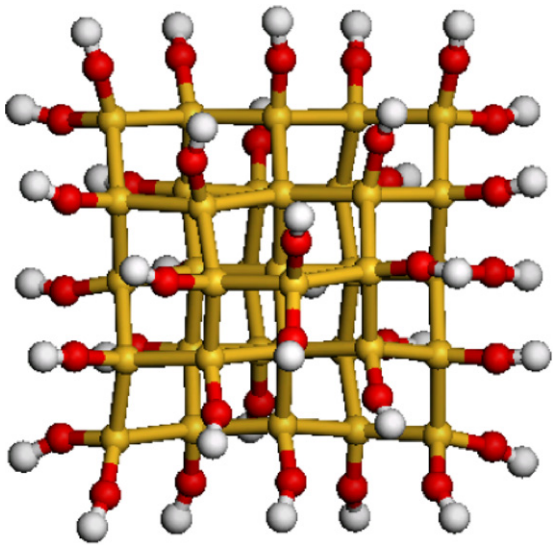

Figure 2. Structure of cluster $Si_{35}(OH)_{36}$.

to twice the β cristobalite theoretical lattice constant. Then, we remove from the supercell center 12 oxygen atoms to form a Si-rich region which contains 10 silicon atoms. Thereby, a small nc-Si (called $Si_{10}(2 \times 2 \times 2)$) is now surrounded by a crystalline SiO_2 matrix. The resulting supercell contains 64 Si atoms and 116 O atoms. The diameter of the nc-Si is about 7 Å.

3.2. $Si_{10}(3 \times 3 \times 3)$

The previous nc-Si (model 3.1) is now created in the center of a $3 \times 3 \times 3$ supercell whose cell side is three times the β cristobalite lattice constant. 12 oxygen atoms are removed from the supercell. The structure contains 216 silicon atoms and 420 oxygen atoms. With this Si_{10} $(3 \times 3 \times 3)$ model, we want to study the influence of the nanograin density on the nanocrystal electronic and optical properties, since intergrain distance is greater than in the preceding model 3.1.

3.3. $Si_{35}(3 \times 3 \times 3)$

We design a $3 \times 3 \times 3$ supercell, then remove 52 O atoms from the center. There is a silicon-rich region containing 35 silicon atoms surrounded by β cristobalite. The 35 atom nc-Si diameter is twice as large as nc-Si in the model $Si_{10}(2 \times 2 \times 2)$.

3.4. nc-Si with interface defects

It is well known that the Si/SiO_2 interface structure consists of intermediate formal oxidation states, i.e. Si^{1+}, Si^{2+} and Si^{3+}. This may lead to two kinds of interface bonds which can be considered as interface defects: the Si=O double bond and the Si–O–Si bridge bond where one oxygen atom links two silicon atoms of nc-Si.

Si_{11}=O nanograin: in order to simulate a Si=O double bond, we have inserted at the surface of the $Si_{10}(2 \times 2 \times 2)$ nanograin one Si–O couple between two Si atoms.

$Si_{10}O$ nanograin: Si–O–Si bridge bonds at the nc-Si/SiO_2 interface have been simulated by the Monte Carlo method [13]. The authors [13] have calculated the percentage of bridge bonds in several nc-Si/SiO_2 systems. By extrapolating their results, we have found that the percentage of bridge bonds is evaluated to be 10% in the 5 Å nc-Si. Thus, we have inserted only one bridge bond, choosing one site among 12 possibilities at the nc-Si/SiO_2 interface.

3.5. Isolated nc-Si

We create isolated nc-Si to realize the cluster calculations using LDA-AIMPRO code or B3LYP-CRYSTAL06 code. From the relaxed atomic structures of $Si_{10}(2 \times 2 \times 2)$, $Si_{35}(3 \times 3 \times 3)$, Si_{11}=O and $Si_{10}O$ systems, we extract all Si atoms of the nanograin and their first neighbor oxygen atoms. The first type of cluster is produced by replacing the O atoms by H atoms and by setting the Si–H distance to 1.5 Å. With this approach, we obtain a $Si_{10}H_{16}$ cluster. The second type of cluster is produced by adding hydrogen atoms so that the Si–O–H angle is equal to the corresponding Si–O–Si angle at the nc-Si/SiO_2 interface and by setting the O–H distance to 1 Å. With this approach, we obtain four Si clusters $Si_{10}(OH)_{16}$ (figure 1), $Si_{35}(OH)_{36}$ (figure 2), $Si_{11}O_{17}H_{16}$ and $Si_{10}O_{17}H_{16}$.

4. Si nanocrystals

4.1. Atomic structure of nc-Si

The three supercells containing $Si_{10}(2 \times 2 \times 2)$, $Si_{10}(3 \times 3 \times 3)$ and $Si_{35}(3 \times 3 \times 3)$ are totally relaxed. We present the final structure of the $Si_{35}(3 \times 3 \times 3)$ nanograin in figure 3.

The final average Si–Si bond length between Si atoms of nc-Si in these three models is about 2.4 Å, +6% with respect to the value optimized for crystalline silicon. The equilibrium supercell parameters are reduced by 7% in the $Si_{10}(2 \times 2 \times 2)$ supercell, 5% in the $Si_{10}(3 \times 3 \times 3)$ supercell and 8% in

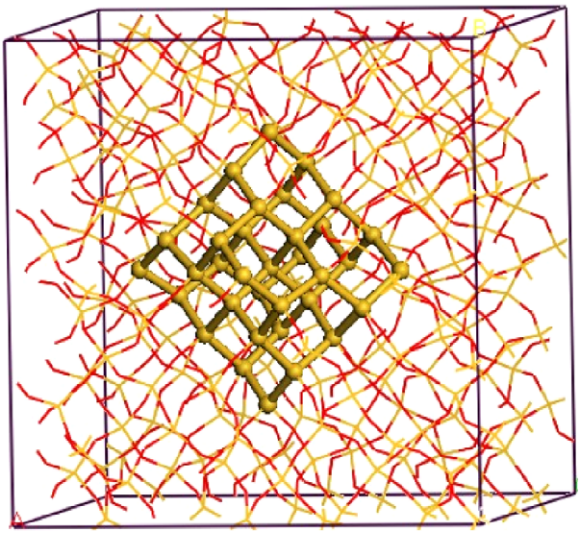

Figure 3. Final structure of $Si_{35}(3 \times 3 \times 3)$.

the $Si_{35}(3 \times 3 \times 3)$ supercell with respect to the theoretical parameter optimized for a supercell of pure β-SiO_2.

In a region which extends over 3 Å from the nanograin surface, the Si–O distance between a Si atom of nc-Si and an interface O atom is distributed from 1.63 to 1.66 Å and the Si–O–Si angle at the interface is distributed from 158° to 175°. Deep in the SiO_2 matrix, the Si–O distance is smaller (between 1.6 and 1.61 Å) and the Si–O–Si angle becomes smaller (between 136° and 149°). These values (Si–O distance and Si–O–Si angle) in the matrix are very similar to those in amorphous SiO_2 [10]. Thus we can evaluate the interface thickness to 3 Å. With DFT calculations on a plane Si/SiO_2 interface, Neaton *et al* [33] proposed 5 Å.

4.2. Influence of the mean distance between nanograins

We have designed a nanocrystal containing 10 Si atoms in a $2 \times 2 \times 2$ supercell and in a $3 \times 3 \times 3$ supercell to study the influence of the mean distance between nanograins on electronic and optical properties of nc-Si/SiO_2.

After total relaxation, the $Si_{10}(2\times2\times2)$ and $Si_{10}(3\times3\times3)$ nanograins have the same diameter, which is equal to 5.6 Å, whereas the intergrain distance is half the size in the $(2\times2\times2)$ supercell that it is in the $(3 \times 3 \times 3)$ supercell. By calculating the formation energy, we found that the system is more stable as the distance between nanograins increases.

Both the band structure and electronic densities of these nc-Si systems are very similar. This result supports the conclusion that a nanograin distance of about 8 Å is large enough that there is no interaction between nanograins.

By calculating EELS of these two nc-Si systems, we have found that the absorbance of nc-Si_{10} in the $(2\times2\times2)$ supercell is more efficient than in the $(3 \times 3 \times 3)$ supercell, where the nanograin density is three times smaller. The absorption peak at around 6 eV for $(2 \times 2 \times 2)$ system is six times more intense than that of the $(3 \times 3 \times 3)$ system. We can conclude that the absorbance of nc-Si is proportional to the nanograin density in the system.

The band structure is characteristic of a semiconductor (figure 4). We have found the LDA gap equal to 2 eV, which is much smaller than that of β cristobalite (6.15 eV). The strong reduction is caused by the introduction of some specific levels within the SiO_2 band gap due to the presence of the Si nanograin. Deep inside the conduction and valence bands of SiO_2, the typical behavior of the β cristobalite bulk is still recognizable. The indirect LDA band gap shifts from 0.64 eV in bulk silicon to 2 eV for an nc-Si of 5.6 Å in diameter. The gap becomes more direct since both valence and conduction bands are 'flatter' in the case of Si nanograins than in the case of bulk Si. This band gap is very similar to the result of Daldosso *et al* [2], where a GGA-PBE energy gap of 2.07 eV (1.96 eV in LDA) was obtained.

4.3. Influence of the matrix

We present here the influence of the matrix on the atomic structure and on the energy gap of the nanograin. On the basis of the AIMPRO relaxed nc-Si/SiO_2 supercell, we have thus extracted nc-Si clusters. The saturation of the dangling bond leads to two types of molecules (see section 3.5). The calculations are performed here on the $Si_{10}H_{16}$ cluster (figure 1) using the LDA-AIMPRO code. The silicon

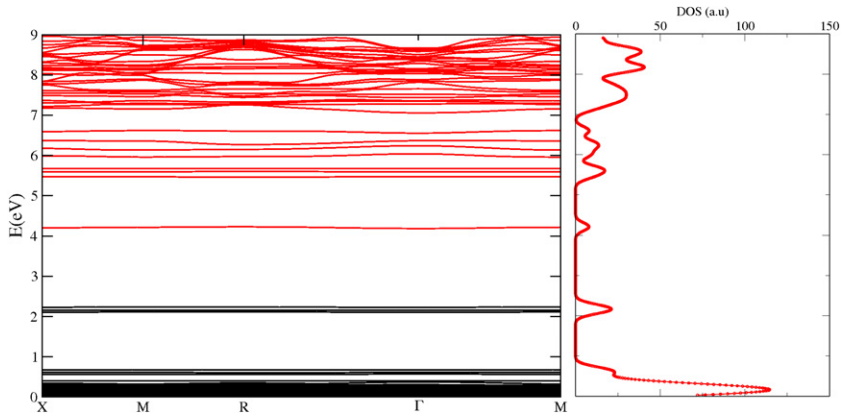

Figure 4. Band structure and density of states of $Si_{10}(2 \times 2 \times 2)$.

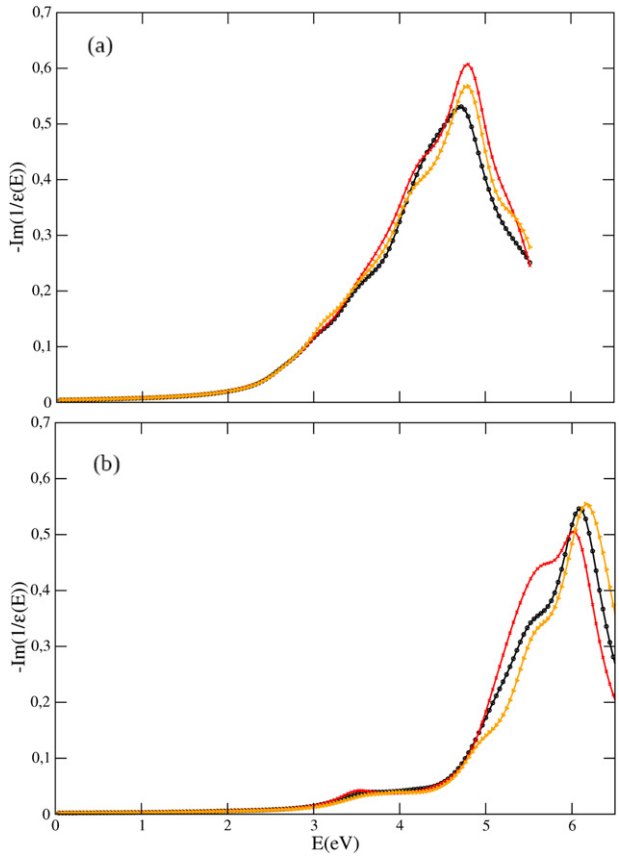

Figure 5. Absorption spectrum of nc-Si: (a) $Si_{35}(3 \times 3 \times 3)$ and (b) $Si_{10}(2 \times 2 \times 2)$.

cluster shape is spheroidal (see section 3.5) and the LDA HOMO/LUMO energy difference is evaluated to be 5.1 eV. At the second step, we relax the structure of the cluster, the shape of the silicon cluster changes into oblate form and the LDA HOMO/LUMO energy difference is evaluated as 4.7 eV. These values are much greater than that of nc-Si/SiO_2 (2 eV, see section 4.2). We can conclude that the matrix influences both the shape and the electronic properties of nc-Si.

Since the LDA HOMO/LUMO energy difference of the $Si_{10}H_{16}$ cluster is much larger than the energy gap of the nc-Si/SiO_2 supercell, the use of such a hydrogenated cluster does not seem relevant to describe a nanograin in the SiO_2 matrix. In the case of the $Si_{10}(OH)_{16}$ cluster (figure 1) and the $Si_{35}(OH)_{36}$ cluster (figure 2), the LDA HOMO/LUMO energy differences are very close to the values obtained on supercell calculations. It seems sufficient to take into account only the first neighbor oxygen atoms in the case of a cluster calculation in order to reproduce the supercell calculations and to propose a realistic model.

4.4. Influence of nanograin size

Since the distance between the nanograin boundaries is the same in $Si_{10}(2 \times 2 \times 2)$ and $Si_{35}(3 \times 3 \times 3)$ systems, we have a means to investigate only the influence of the nanograin size.

We find that the Kohn–Sham band gap of the Si_{35} nanograin (diameter 11 Å) is smaller than that of the Si_{10} nanograin (diameter 5.6 Å). In our calculations, the nc-Si energy gap increases with decreasing grain size in accordance with the quantum confinement concept.

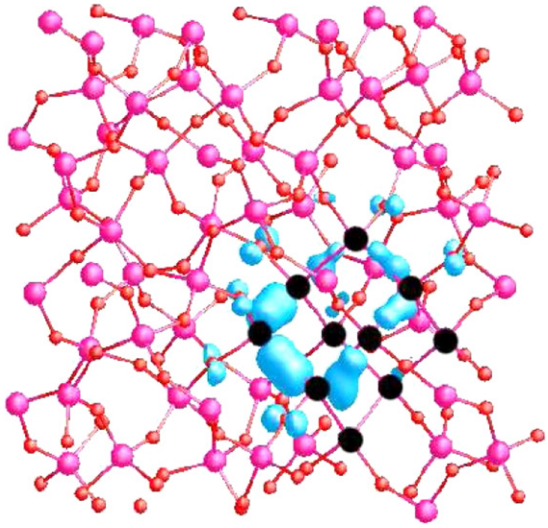

Figure 6. Square modulus of HOMO-$Si_{10}(2 \times 2 \times 2)$.

An efficient approach to improve the description of the band gap is to use the B3LYP approximation [34], which is implemented in the CRYSTAL06 code. Thus we use this code on the $Si_{10}(OH)_{16}$ and $Si_{35}(OH)_{36}$ clusters. For the smaller cluster (5.6 Å, $Si_{10}(OH)_{16}$) the B3LYP gap is equal to 3.4 eV, while that of the larger one (11 Å, $Si_{35}(OH)_{36}$) is equal to 3.1 eV. Our results are in accordance with the optical energy gap measured by absorption spectroscopy. Kim *et al* [35] have obtained optical gaps of 3.04, 2.61 and 2.12 eV for nc-Si whose diameters are respectively equal to 10, 22 and 30 Å.

The absorption spectra $-\mathrm{Im}(\epsilon(E)^{-1})$ of these 5.6 and 11 Å diameter nc-Si are plotted in figure 5. Because nc-Si is not really isotropic, the dielectric constant is a 3×3 matrix. Here, the absorption spectra contain three curves corresponding to the diagonal values ϵ_x, ϵ_y and ϵ_z. The larger nc-Si produces a redshift in the optical absorption spectrum with respect to the 5.6 Å nc-Si. This result is again in accordance with the quantum confinement concept.

4.5. Electronic density in 3D

We present here the electronic density of two nc-Si/SiO_2 systems. We know that the DFT calculations give only Kohn–Sham orbitals. However, from the spatial distribution of these orbitals, we can obtain a qualitative representation of the electron localization in 3D. For the $Si_{10}(2 \times 2 \times 2)$, the spatial distribution of the HOMO (figure 6) is mainly localized on the Si atoms of nc-Si. A weaker presence probability is obviously observed on the O atoms at the nc-Si/SiO_2 interface. The orbital localization on the nc-Si region supports the view of near-band-edge states related to nc-Si, while the contribution on the O atoms indicates the role of the silica matrix on the nc-Si level organization suggested by the band structure analysis. This can lead to the conclusion that the transition region around nc-Si can participate in the optical activity on the

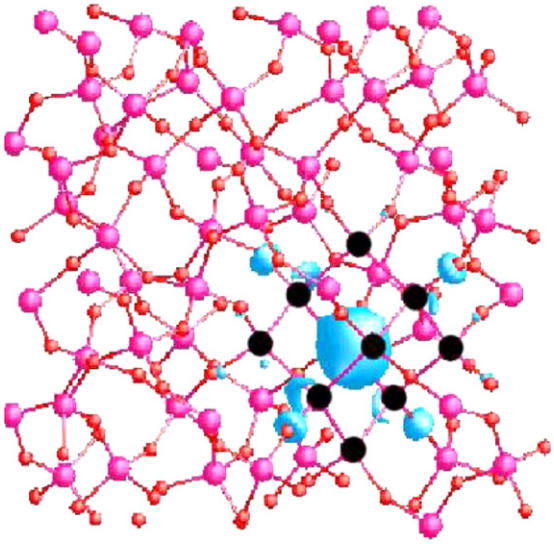

Figure 7. Square modulus of LUMO-$Si_{10}(2 \times 2 \times 2)$.

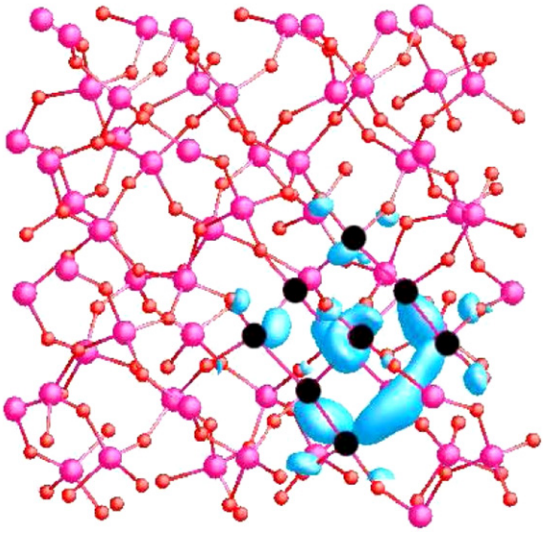

Figure 8. Square modulus of LUMO+1-$Si_{10}(2 \times 2 \times 2)$.

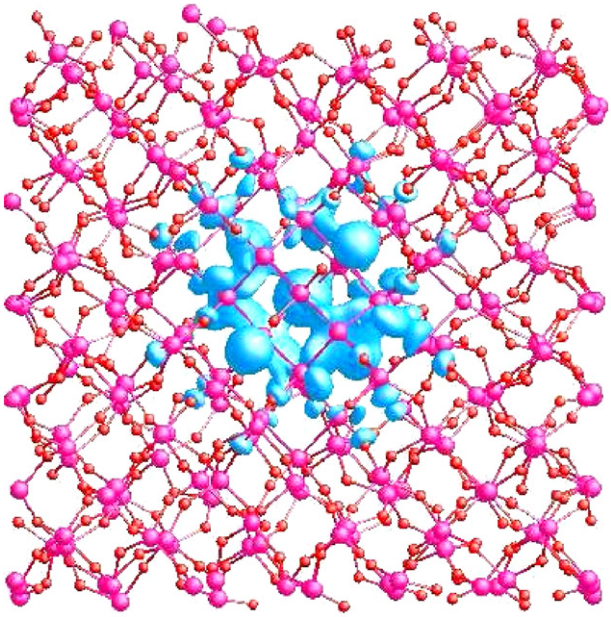

Figure 9. Square modulus of LUMO-$Si_{35}(3 \times 3 \times 3)$.

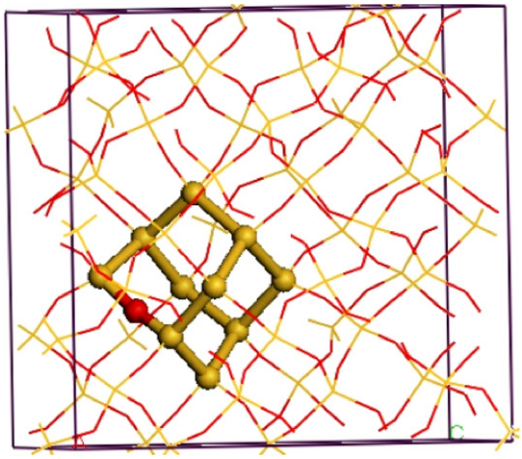

Figure 10. Final structure of $Si_{10}O$.

system. The LUMO of $Si_{10}(2 \times 2 \times 2)$ shows a totally different behavior: the distributions tend to be localized mostly inside the nanograin and on some oxygen atoms at the nc-Si surface (figure 7). The LUMO+1 level is the first unoccupied orbital at energies higher than the LUMO (figure 8). The corresponding distributions are localized at the nc-Si/SiO_2 interface. In the spectrum of 5.6 Å nc-Si (figure 5), we consider the absorption corresponding to photon energy lower than 4 eV. We see one peak centered at 3.4 eV, which is mainly due to HOMO–LUMO + 1 transition. This peak is much more intense than the peak around 2 eV associated with the HOMO–LUMO transition. So, we can conclude that there are possibilities of formation of excitons (electron–hole pairs) at the nc-Si/SiO_2 interface.

For the nc-Si_{35}, the HOMO distribution has the same behavior as that of nc-Si_{10}. The LUMO distribution tends to be localized not only inside the nanograin but also on the Si atoms at the nc-Si/SiO_2 interface (figure 9). We can conclude that when the nc-Si/SiO_2 system is excited the electron seems to be found at the interface of nc-Si and the matrix.

5. Role of interface defects on the electronic properties of nc-Si in SiO_2

After total relaxation, we get the final structures of two types of nanograins: $Si_{10}O$ (figure 10) and Si_{11}=O (figure 11). In these two models, the final Si–Si bond length between Si atoms of nc-Si and the equilibrium supercell parameter are the same as those of $Si_{10}(2 \times 2 \times 2)$. The interface region is about 3 Å wide, the same value as that of $Si_{10}(2 \times 2 \times 2)$. In the Si_{11}=O nanograin, the bond length of the Si=O double bond is equal to 1.528 Å. This value is similar to the result of silicon cluster calculations for the $Si_{10}H_{14}O$ molecule: 1.529 Å [17] and 1.524 Å [16].

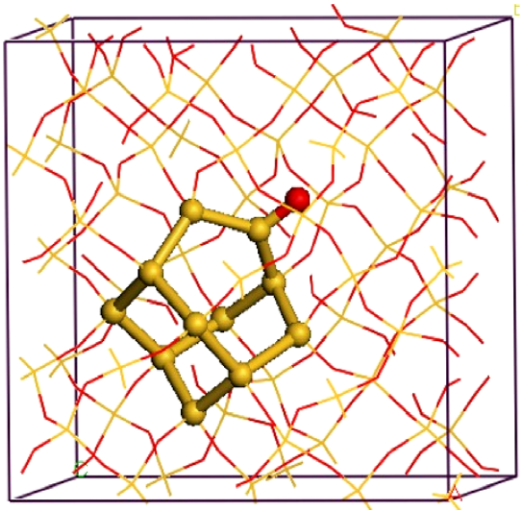

Figure 11. Final structure of Si_{11}=O.

The formation energies of the three nc-Si/SiO_2 systems, $Si_{10}(2 \times 2 \times 2)$ (see section 3.1), $Si_{10}O$ and Si_{11}=O (see 3.4), are found to be 9.8, 8.7 and 13 eV, respectively. So, the $Si_{10}O$ nanograin with Si–O–Si bridge bond at the interface is the most stable configuration. Gatti *et al* [17] have found that the cluster surface with one Si–O–Si bridge bond leads to the most stable structure. We can conclude that the presence of a Si–O–Si bridge bond at the nc-Si surface favors the stability of the system whatever the configuration (nc-Si cluster or nc-Si embedded in a silica matrix).

The electronic properties of the $Si_{10}O$ and Si_{11}=O nanograins are characterized by the interface defects. The B3LYP band gap of $Si_{10}O$ is equal to 3.6 eV while that of Si_{11}=O is equal to 3.3 eV. By creating interface defects, we have modified the energy gap of the nanograin; the Si–O–Si bridge bond increases the gap while the Si=O double bond reduces the gap. This finding is in accordance with the conclusion of Luppi *et al* [16], who have investigated the multiple Si=O bonds at the silicon molecule surface. So we can conclude that the presence of Si=O bonds at either the silicon cluster surface or the nc-Si/SiO_2 interface reduces the energy gap.

The electronic density of $Si_{10}O$ is very similar to that of $Si_{10}(2 \times 2 \times 2)$. The role of oxygen atoms at the nc-Si/SiO_2 interface is once again confirmed by the spatial electronic distribution on the O atom of the Si–O–Si bridge bond. The HOMO–LUMO transition relates to the interface defects.

6. Conclusion

We have used first-principle calculations to study the atomic and electronic structures of nc-Si/SiO_2 systems (Si nanograins embedded in SiO_2 β cristobalite) and the influence of parameters such as the nanograin size, the mean distance between the nanograins and the presence of defects at the nc-Si/SiO_2 interface. We have calculated the absorption spectrum of nc-Si/SiO_2 systems. The band gap of nc-Si is more direct than that in bulk silicon because of a 'flattening' of the valence and conduction bands. Our results are in accordance with the quantum confinement concept: as the nanograin size is reduced we observe an energy gap increase and a blueshift in the absorption spectrum. The B3LYP energy gaps of 5.6 and 11 Å nc-Si are respectively equal to 3.4 and 3.1 eV. The system is more stable as the distance between nanograins increases or in other words as the nanograin density decreases. The nc-Si/SiO_2 interface defects influence the electronic properties (energy gap). We find that the system with Si–O–Si bridge bonds at the interface is the most stable configuration and the Si=O double bond reduces the energy gap and causes a redshift in the absorption spectrum.

Acknowledgments

The computations were performed at CRIHAN (Centre de Ressources Informatiques de Haute Normandie-Rouen, France) and at CINES (Centre Informatique National de l'Enseignement Supérieur Montpellier, France).

References

[1] Canham L T 1990 *Appl. Phys. Lett.* **57** 1046
[2] Daldosso N, Luppi M, Ossicini S, Degoli E, Magri R, Dalba G, Fornasini P, Grisenti R, Rocca F, Pavesi L, Boninelli S, Priolo F, Spinella C and Iacona F 2003 *Phys. Rev.* B **68** 085327
[3] Ternon C, Gourbilleau F, Portier X, Voivenel P and Dufour C 2002 *Thin Solid Films* **419** 5
[4] ShimizuIwayama T, Terao Y, Kamiya A, Takeda M, Nakao S and Saitoh K 1996 Visible photoluminescence from silicon nanocrystals formed in silicon dioxide by ion implantation and thermal processing *Thin Solid Films* **276** 104–7
[5] Pellegrino P, Garrido B, Garcia C, Arbiol J, Morante J R, Melchiorri M, Daldosso N, Pavesi L, Scheid E and Sarrabayrouse G 2005 Low-loss rib waveguides containing Si nanocrystals embedded in SiO_2 *J. Appl. Phys.* **97** 074312
[6] Lu Z H, Lockwood D J and Baribeau J-M 1995 Quantum confinement and light emission in SiO_2/Si superlattices *Nature* **378** 258–60
[7] Wilcoxon J P, Samara G A and Provencio P N 1999 *Phys. Rev.* B **60** 2704
[8] Pavesi L, Negro L, Mazzoleni C, Franzo G and Priolo F 2000 *Nature* **408** 440
[9] Takeoka S, Fujii M and Hayashi S 2000 *Phys. Rev.* B **62** 16820
[10] Yamashita Y, Yamamoto S, Mukai K, Yoshinobu J, Harada Y, Tokushima T, Takeuchi T, Takata Y, Shin S, Akagi K and Tsuneyuki S 2006 *Phys. Rev.* B **73** 045336
[11] Ming Z, Nakajima K, Suzuki M, Kimura K, Uematsu M, Torii K, Kamiyama S, Nara Y and Yamada K 2006 *Appl. Phys. Lett.* **88** 153516
[12] Proot J P, Delerue C and Allan G 1992 *Appl. Phys. Lett.* **61** 1948
[13] Hadjisavvas G and Kelires P C 2004 *Phys. Rev. Lett.* **93** 226104
[14] Djurabekova F and Nordlund K 2008 Atomistic simulation of the interface structure of Si nanocrystals embedded in amorphous silica *Phys. Rev.* B **77** 115325
[15] Onida G and Andreoni W 1995 *Chem. Phys. Lett.* **243** 183
[16] Luppi M and Ossicini S 2003 *J. Appl. Phys.* **94** 2130
[17] Gatti M and Onida G 2005 *Phys. Rev.* B **72** 045442

[18] Luppi E, Iori F, Magri R, Pulci O, Ossicini S, Degoli E and Olevano V 2007 *Phys. Rev.* B **75** 033303
[19] Hadjisavvas G and Kelires P C 2007 *Physica* E **38** 99
[20] Delerue C, Allan G and Lannoo M 1993 *Phys. Rev.* B **48** 11024
[21] Delerue C, Lannoo M and Allan G 2000 Excitonic and quasiparticle gaps in Si nanocrystals *Phys. Rev. Lett.* **84** 2457
[22] Jones R and Briddon P R 1998 *The Ab initio Cluster Method and the Dynamics of Defects in Semiconductors* vol 51A (New York: Academic)
[23] Jones R and Briddon P R 1997 *Semiconductors and Semimetals: Identification of Defects in Semiconductors* (New York: Academic)
[24] Hartwigsen C, Goedecker S and Hutter J 1998 *Phys. Rev.* B **58** 3641–62
[25] Wyckoff W L 1925 *Am. J. Sci.* **9** 448
[26] Lide D R 1992 *Handbook of Chemistry and Physics* (Boca Raton, FL: CRC Press)
[27] Monkhorst H J and Pack J D 1976 *Phys. Rev.* B **13** 5188
[28] Fall C J, Blumenau A T, Jones R, Briddon P R, Frauenheim T, Gutierrez-Sosa A, Bangert U, Mora A E, Steeds J W and Butler J E 2002 *Phys. Rev.* B **65** 205206
[29] Eberlein T A G, Jones R and Briddon P R 2003 *Phys. Rev. Lett.* **90** 225502
[30] Dovesi R, Saunders V R, Roetti C, Orlando R, Zicovich-Wilson C M, Pascale F, Civalleri B, Doll K, Harrison N M, Bush I J, D'Arco P and Llunell M 2006 *CRYSTAL-06 User's Manual* Universitá di Torino
[31] Nada R, Catlow C R A, Dovesi R and Pisani C 1990 An *Ab initio* Hartree–Fock study of alpha-quartz and stishovite *Phys. Chem. Minerals* **17** 353–62
[32] Civalleri B, Casassa S, Garrone E, Pisani C and Ugliengo P 1999 *J. Phys. Chem.* B **103** 2165
[33] Neaton J B, Muller D A and Ashcroft N W 2000 *Phys. Rev. Lett.* **85** 1298
[34] Muscat J, Wander A and Harrison N M 2001 *Chem. Phys. Lett.* **342** 397
[35] Kim K, Suh M S, Oh D H, Lee Y H, Youn C J, Lee K B and Lee H J 1997 *J. Korean Phys. Soc.* **30** 580